


ORIGINAL ARTICLE

CircFOXM1 acts as a ceRNA to upregulate SMAD2 and promote the progression of nasopharyngeal carcinoma

Shuai Pei^{1,2}  | Chengxian Ma² | Jie Chen² | Xinyu Hu² | Mingyu Du² | Tian Xu² | Mengna Zhan² | Ke Xue² | Yufeng Zhang² | Li Yin² | Xia He^{1,2}¹Xuzhou Medical University, Xuzhou, Jiangsu, China²Jiangsu Cancer Hospital, Jiangsu Institute of Cancer Research, Nanjing Medical University Affiliated Cancer Hospital, Nanjing, Jiangsu, China**Correspondence**Xia He, Xuzhou Medical University, Xuzhou, Jiangsu, China
Email: hexiabm@163.comLi Yin, Jiangsu Cancer Hospital, Jiangsu Institute of Cancer Research, Nanjing Medical University Affiliated Cancer Hospital, Nanjing, Jiangsu, China.
Email: yinli_2012@126.com**Funding information**

China Postdoctoral Science Foundation, Grant/Award Number: 2020M671398; National Natural Science Foundation of China, Grant/Award Number: 81702685, 8187101501 and 82003223; National Science Foundation of China

Abstract

Background: In recent years, the development of high-throughput sequencing technology has promoted the rapid development of circRNA-related research. Studies have found that circRNA plays a key role in a variety of tumors, but few people study the role of circRNA in nasopharyngeal carcinoma. Under comprehensive treatments, the 5-year survival rate can reach about 70%, but some patients still have distant metastases or recurrences after treatment. Therefore, it is very important to study the molecular mechanisms of the proliferation and invasion of nasopharyngeal carcinoma.

Methods: QRT-PCR was applied to detect the relative expression level of circFOXM1 in NPC and nasopharyngeal epithelial cell lines. We knocked down circFOXM1 and studied the influence of circFOXM1 on NPC cells. Nuclear and cytoplasmic RNA isolation experiments, fluorescence in situ hybridization (FISH), bioinformatics analysis, the dual-luciferase reporter experiment, Western Blot, and other experiments were conducted to verify the relationships among circFOXM1, miR-136-5p, and SMAD2. We collected clinical NPC samples to prove the effect of circFOXM1 on the prognosis and treatment of NPC.

Results: In this study, we found that circFOXM1 is highly expressed in nasopharyngeal carcinoma tissue cells compared with adjacent normal tissues and is related to the staging of nasopharyngeal carcinoma. High expression of circFOXM1 indicates a poor prognosis for nasopharyngeal carcinoma. Knockdown of CircFOXM1 inhibited the proliferation and invasion of nasopharyngeal carcinoma cells.

Conclusion: CircFOXM1 promotes the malignant proliferation of nasopharyngeal carcinoma cells by regulating the miR-136-5p-SMAD2 axis.

KEYWORDS

ceRNA, circFOXM1, invasion, migration, miR-136-5p, NPC

Shuai Pei, Chengxian Ma and Jie Chen contributed equally to this work.

This is an open access article under the terms of the Creative Commons Attribution-NonCommercial-NoDerivs License, which permits use and distribution in any medium, provided the original work is properly cited, the use is non-commercial and no modifications or adaptations are made.

© 2022 The Authors. *Molecular Genetics & Genomic Medicine* published by Wiley Periodicals LLC.

1 | INTRODUCTION

Nasopharyngeal carcinoma (NPC) is a typical head and neck malignant tumor originating from the human nasopharyngeal mucosal epithelium, with a relatively high degree of malignancy. The incidence rate is relatively high in Asia and North Africa (Chua et al., 2016). Genetic factors, environmental factors, Epstein–Barr virus (EBV) infection, and other factors promote the development of NPC (He et al., 2017). Due to the insidious symptoms, the aggressiveness of the tumor, and insufficient patient cognition, most patients with NPC are already in the advanced stage at the time of diagnosis (Lai et al., 2011; Lee et al., 2015). Although with the development of radiotherapy technology in recent decades, the 5-year survival rate of NPC remained reaches about 70% under the comprehensive treatment based on radiotherapy. Tumor recurrence or distant metastasis still occurred within a few years after treatment. It is the main reason for treatment failure of some patients (Li et al., 2017). Therefore, it is particularly important to study the potential molecular mechanism of the occurrence and development of NPC and to provide better biomarkers for the early diagnosis and treatment of NPC.

Noncoding RNA includes long-chain noncoding RNA (lncRNA), microRNA (miRNA), and circular RNA (circRNA). CircRNA originates from exons, introns, or intergenic regions (Qu et al., 2017), the 5' head and 3' end of RNA mainly through reverse shearing head to end to form a covalent bond to form a closed-loop structure (Ebbesen et al., 2016). In recent years, with the development of high-throughput sequencing technology, circRNA has been discovered in large numbers, opening a new era of circRNA research. According to research, the biological functions of circRNA mainly include miRNA sponge function, namely ceRNA, regulating protein binding, encoding a synthetic protein, regulating parent gene expression, and so on. In 2011, Leonardo Salmena et al. proposed the competitive endogenous RNA (ceRNA) hypothesis (Salmena et al., 2011), revealing the regulatory role of ceRNA in the process of transcription, enriching the genetic information of the human genome, and playing a significant role in the pathogenesis and progress of cancer and other diseases (Qu et al., 2015).

Accumulating evidence have found that abnormally expressed microRNA or lncRNA plays an indispensable role in promoting tumorigenesis and development in NPC (Mai et al., 2019; Zheng et al., 2019). The role of circRNA in other tumors has been studied. CircRNA- has miRNA-binding sites that regulate downstream gene expression. Many studies have reported that circRNA can serve as a “microRNA sponge” to regulate downstream gene expression. Luo Zai et al. found that circCCDC9 acts as a

miR-6792-3p sponge and regulates the expression of *CAVI* (OMIM accession number: 601047) to inhibit the progression of gastric cancer (Luo et al., 2020). Liu Zhenguo et al. found that CircRNA-5692 adsorbed miR-328-5P to enhance the expression of *DAB2IP* (OMIM accession number: 609205) to inhibit the progression of hepatocellular carcinoma (Liu et al., 2019).

However, the biological function of circRNA in the occurrence and development of NPC is still rarely studied. In this study, our experimental group found that circFOXM1 (hsa_circ_0025042) originates from chr12: 2983142 to 2983691 and is highly expressed in NPC cells. We first proved the ring structure of circFOXM1 and then verified that circFOXM1 is abnormally highly expressed in NPC cell lines compared with nasopharyngeal normal tissue cells, related to the staging and poor prognosis of NPC, and determined circFOXM1 overexpression effectively enhance the malignant behavior of NPC. In addition, we searched the database and found its potential target miR-136-5p, and miR-136-5p inhibits EMT (Epithelial-Mesenchymal Transition) by targeting *SMAD2* (OMIM accession number: 601366) to exert a tumor suppressor effect (Yang et al., 2013). It was found that circFOXM1 adsorbed miR-136-5p through the ceRNA mechanism, which restricted the binding of miR-136-5p and inhibited the expression of *SMAD2*, then promoted the EMT of NPC, and ultimately facilitated the proliferation and invasion of NPC.

2 | MATERIALS AND METHODS

2.1 | Patients and samples

A total of 8 normal nasopharyngeal epithelial tissues and 40 frozen NPC tissues were gathered from the Radiation Therapy Center of Jiangsu Cancer Hospital (Nanjing, China). All the patients contained in the study signed informed consent. All tissue samples were confirmed by pathology, and Jiangsu Cancer Hospital Ethics Review Committee had approved these clinical samples and the study.

2.2 | Cell culture

The Radiation Therapy Laboratory of Jiangsu Cancer Hospital supplied seven human NPC cell lines (SUNE1, CNE1, HNE1, CNE2, 5-8F, 6-10B, and C666) and a human normal nasopharyngeal epithelial cell line (NP69). In these cell lines, SNE1, CNE1, HNE1, CNE2, 5-8F, 6-10B, and C666 were cultivated in FMI 1640 (Corning, USA) added with 10% fetal bovine serum (FBS; Gibco, USA).

NP69 was cultivated in serum-free medium (Invitrogen) added to bovine pituitary extract (BD Biosciences). All cell lines were cultured in 5% CO₂ and humid air at 37°C.

2.3 | RNA extraction and qRT-PCR

Total RNA was obtained from clinical samples or NPC cells using TRizol reagent (Invitrogen) according to the experiment manual. The nuclear and cytoplasmic segregations were obtained with NE-PER Nuclear and Cytoplasmic Extraction Reagents (Thermo Scientific, USA).

The complementary DNA (cDNA) was synthesized from circRNA, mRNA, and total RNAs by using a reverse transcription kit (Takara, Japan). QRT-PCR reactions were carried out on a 7500 FAST real-time PCR machine (Applied Biosystems) utilizing SYBR Green PCR Master Mix. U6 and GAPDH served as standardized controls. The sequences of all primers were listed in the Table S1.

2.4 | Plasmid construction

Si-circFOXM1 and negative controls were purchased from Ribobio (Guangzhou, China). MiR-136-5p mimics and inhibitors were commercially designed and synthesized at Genechem (Shanghai, China). To overexpress *SMAD2*, the open reading frames (ORFs) of *SMAD2* are amplified by PCR and inserted into the pcDNA3.1 (+) and pcDNA3.1 plasmid (V79020) bought from Invitrogen (Carlsbad, CA, USA) following the manufacturer's manual.

2.5 | Transfection

RiboBio (Guangzhou, China) designed and synthesized the miR-136-5p mimics, inhibitors, negative controls, and Si-circ-FOXM1 and siRNA negative controls (si-NC). Cell transfection assay was carried out utilizing Lipofectamine 2000 reagent (Invitrogen, CA, USA) based on the user's manual. Transfected cells were harvested for cell function experiments and qRT-PCR analysis 48 hr after transfection.

2.6 | CCK-8 assay

After transfection, 1×10^3 cells were seeded and incubated in 96-well plates for 1–5 days. Then, 10 μ L CCK-8 reagent (Dojindo, Tokyo, Japan) was added and incubated at 37°C for another 2 hr in the dark. The absorbance values were detected at indicated time points at a wavelength of OD450 nm using a microplate reader (Bio-Rad, USA).

2.7 | Wound-healing assay

Using a sterile pipette tip to create three streaks evenly in each well 24 hr after transfection. Measuring the movement of the cells into the scratch in each well to assess the cell migration. The wound closure speed was observed and photographed to the length at 0 hr after 24 and 48 hr. Each experiment was carried out in triplicate.

2.8 | Determination of colony formation

Colony formation measurement: 800 cells were seeded into six-well plates evenly in 2 mL medium after specific transfection, the cells were cultured for 7–10 days without changing medium. Then, the colonies were washed, fixed, stained, and counted.

2.9 | Trans-well invasion assay

The abilities of cell migration and invasion were detected by the trans-well invasion experiment. NPC cells (103 cells/well) were plated in a serum-free medium in the upper chamber that had been coated with Matrigel. The lower chambers were added with 500 μ L of a medium with 10% FBS. Removing the cells on the upper surface of the top chamber using a cotton swab after 48–72 hr of incubation, and cells that remained on the bottom surface of the top chamber were fixed in 4% paraformaldehyde, stained with 0.1% crystal violet, and counted with an inverted microscope. Experiments were carried out in at least triplicate independently.

2.10 | RNA isolation of nuclear and cytoplasmic fractions

The localization of circFOXM1 in cells was determined using the PARIS kit following the manufacturer's instructions (Ambion, Life Technologies).

2.11 | Western blot analysis

First, each group of cells was harvested, and then proteins were extracted using a lysis buffer. Next, we quantified the proteins with a BCA protein reagent kit (Thermo Scientific, USA). Equal amounts of protein extractions were isolated by SDS-PAGE gels and transferred onto polyvinylidene fluoride (PVDF) membranes at 300 mA for 90 min and incubated overnight with primary antibodies at 4°C (1:1000; Abcam, Cambridge, MA, USA)

against *SMAD2* (ab225958) and β -actin (ab8227). Last, we incubated proteins with the second antibodies (Abcam, ab205718) and analyzed proteins with the ECL plus kit (Beyotime, Haimen, China, P0018S). Images were gained with a BioSpectrum 600 Imaging System (UVP, CA, USA). This experiment was repeated three times and the average value was taken.

2.12 | Statistical analysis

GraphPad Prism 7 and SPSS 23.0 (IBM, SPSS, Chicago, IL, USA) were used to analyze all the experimental data. Student's *t* test or ANOVA was used to analyze the significance between groups. Pearson correlation analysis was performed to assess the correlations between groups. Survival analysis was estimated by the Kaplan–Meier method. The statistical significance criterion was set as a *p* value of $<.05$ ($*p < .05$, $**p < .01$, and $***p < .001$).

3 | RESULTS

3.1 | Characteristics and expression of circFOXM1 in NPC cell lines

In the preliminary experimental screening of the research group, we found that circFOXM1 (hsa_circ_0025042) is abnormally highly expressed in NPC cells. Searching databases such as circBase and circBank found that circFOXM1 is derived from the *FOXM1* (OMIM accession number: 602341) gene of chromosome 12, and its length is 549 bp, formed by the circularization of exon 2 (Figure 1a). Then we selected np69 normal nasopharyngeal cells and six NPC cell lines to detect the expression of circFOXM1 in each cell line using qRT-PCR technology and found that circFOXM1 is highly expressed in NPC 5-8F and 6-10B (Figure 1b). These two cell lines were also selected by us as to subsequent experimental cells. We first designed primers across the circFOXM1 cleavage site and sent the PCR-amplified product for Sanger sequencing. The sequencing results are shown in Figure 1c, indicating that PCR across the circFOXM1 cleavage site can amplify the product, which indicates that circFOXM1 has ring characteristics. Next, we designed forward and reverse primers for the cDNA of circFOXM1 and its parental gene gDNA. Using GAPDH as a reference, PCR amplification was performed. The PCR-amplified products were subjected to DNA gel electrophoresis and found that the cDNA was positive in the two cell lines. The experimental results of reverse primers all have bands, whereas the experimental results of gDNA only forward primers have

bands (Figure 1d), which further proves that it is a circular RNA. RNase digestion experiments show that Rnase can digest linear FOXM1 mRNA, while circFOXM1 is resistant to Rnase (Figure 1e). The reference materials are Actin and GAPDH. In order to probe the location of circFOXM1 in cells, we conducted a nucleocytoplasmic separation experiment to determine the expression levels of circFOXM1, U6, and GAPDH in the nucleus and cytoplasmic components. The qRT-PCR results indicated that about 90% of circFOXM1 is distributed in the cytoplasm (Figure 1f). In this experiment, U6 and GAPDH were used as references. U6 was mainly expressed in the nucleus, and GAPDH was mainly expressed in the cytoplasm. In order to further prove that circFOXM1 is mainly distributed in the cytoplasm, we conducted a FISH experiment. The results are shown in Figure 1g. The quantitative results show that circFOXM1 is mainly distributed in the cytoplasm in 5-8F and 6-10B. Based on the above results, we believe that circFOXM1 is relatively highly expressed in NPC cells and is a circular RNA mainly located in the cytoplasm.

3.2 | Knockdown of circFOXM1 inhibits the proliferation, migration, and invasion of NPC cells

In order to investigate the role of circFOXM1 in NPC cells, si-circFOXM1 was designed. After transfecting cells with si-circFOXM1, RNA was extracted. The results of qRT-PCR revealed that si-circFOXM1 could significantly knock down the expression of circFOXM1 but had no effect on the expression of circFOXM1 parent gene FOXM1 mRNA (Figure 2a). Then we transfected si-NC or si-circFOXM1 into 5-8F and 6-10B cells, respectively, and did a series of functional experiments. The results of CCK8 experiments showed that after knocking down circFOXM1, the proliferation of NPC cells was reduced compared with si-NC (Figure 2b). In the cloning experiment, we tested the inhibitory effect of si-FOXM1-A and si-FOXM1-B on the clonal formation and found that knocking down circFOXM1 inhibits the clonal formation of NPC cells, and the inhibitory effect of si-FOXM1-A is more obvious, and si-FOXM1-A was used in subsequent experiments (Figure 2c). Trans-well results showed that after knocking down circFOXM1 in the two cell lines, the cell invasion ability weakened (Figure 2d). The wound healing showed that after knocking down circFOXM1, the migration ability of NPC cells was suppressed (Figure 2e). The above results reveal that siRNA can significantly knock down the expression of circFOXM1 but does not affect the expression of FOXM1 mRNA; circFOXM1 promotes the proliferation, migration, and invasion of NPC cells.

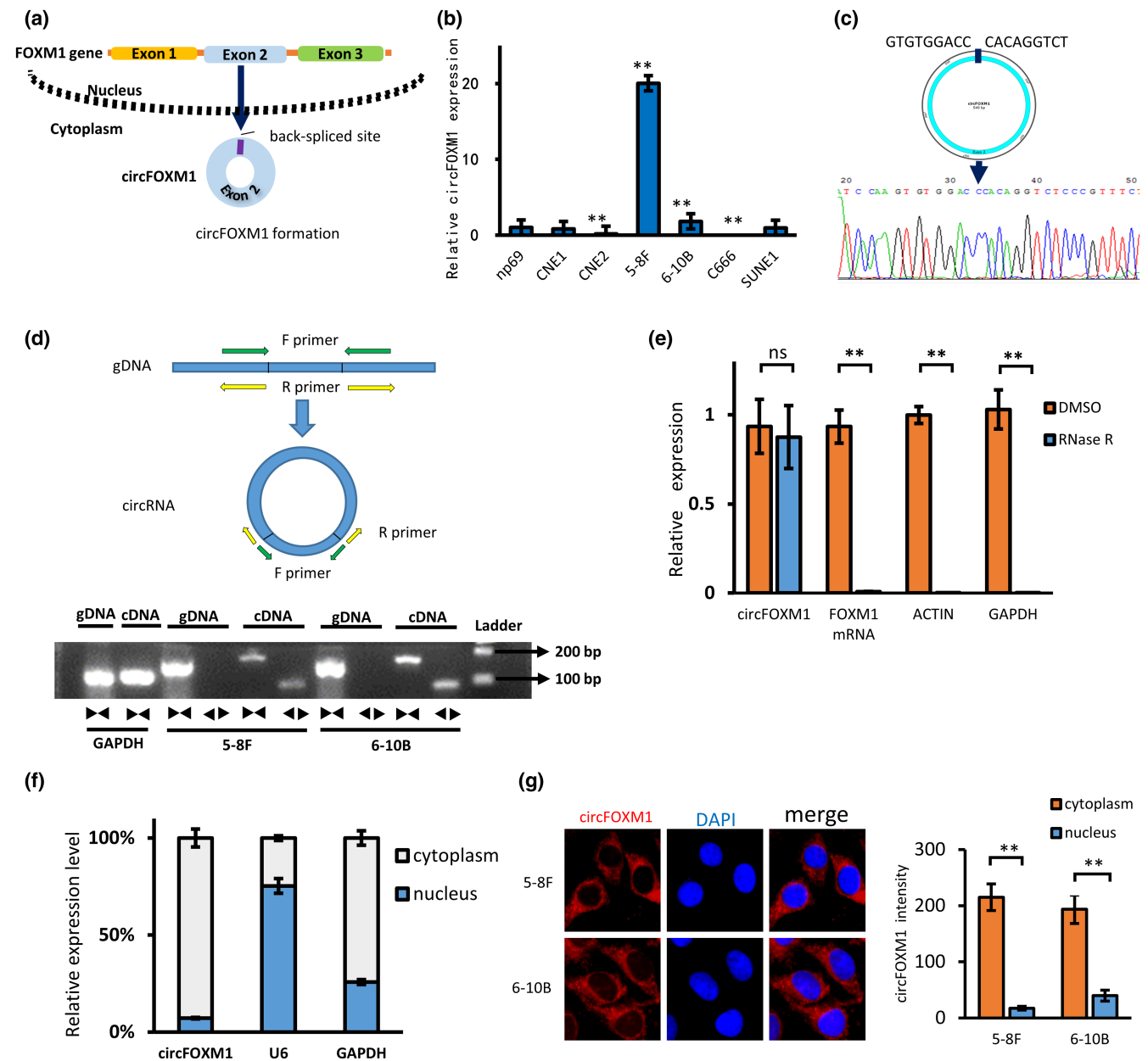


FIGURE 1 Characteristics and expression of circFOXM1 in NPC cell lines. (a) Schematic diagram of the formation of circFOXM1. CircFOXM1 is produced by the circularization reaction of exon 2 of the FOXM1 gene on chromosome 12. (b) The relative expression of circFOXM1 in nasopharyngeal carcinoma cell lines. (c) Sanger sequencing with the RT-PCR product of circFOXM1 to verify the circularity of circFOXM1. (d) The forward and reverse primers for gDNA and circFOXM1 were designed, and the products were amplified by RT-PCR in 5-8F and 6-10B cell lines and then subjected to agarose gel electrophoresis to verify the expression of the products. GAPDH was used as a negative control. (e) qRT-PCR analysis of actin, GAPDH, FOXM1 mRNA, and circFOXM1 expression after RNase R treatment. (f) The relative expression of circFOXM1 in the nucleus and cytoplasm was measured by qPCR. GAPDH serves as a positive control for RNA distributed in the cytoplasm, and U6 serves as a positive control for RNA distributed in the nucleus. (g) FISH showed that circFOXM1 was mainly localized in the cytoplasm. Nuclei were stained with DAPI (blue) and circFOXM1 probes were labeled with Cy3 (red). The error bars (e) represent the SD of three independent experiments. * $p < .05$, ** $p < .01$

3.3 | CircFOXM1 acts as a miR-136-5p sponge in NPC cells

The previous nuclear and cytoplasmic separation experiments have proved that circFOXM1 is mainly located in the cytoplasm. After sequence comparison, circFOXM1

does not have the IRES (inner ribosome entry site) sequence required to encode proteins. Searching the documents, we found that most of the circRNAs located in the cytoplasm play a role by adsorbing miRNAs through the ceRNA mechanism. Therefore, we suspect that circFOXM1 may regulate downstream target gene expression

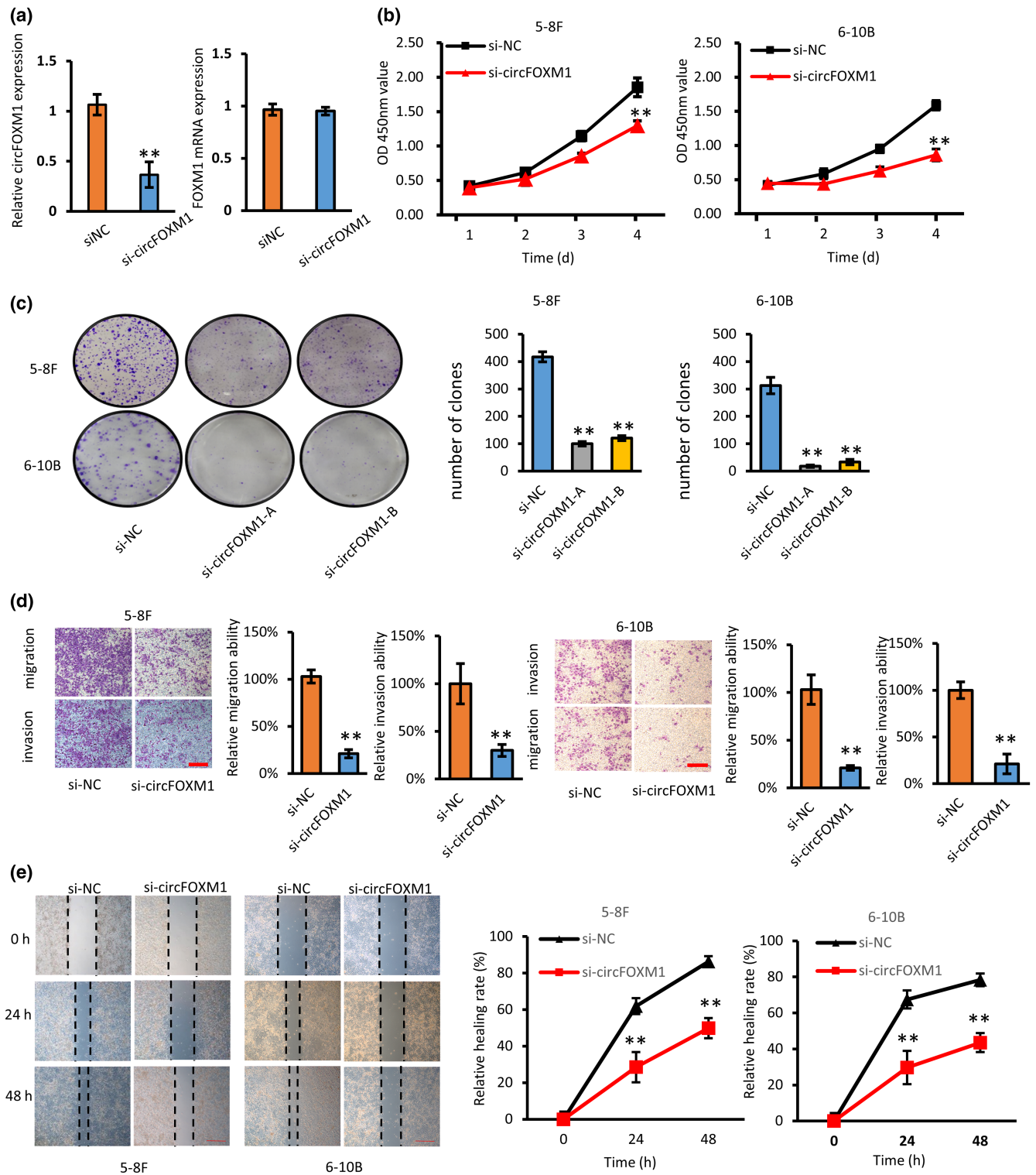


FIGURE 2 circFOXM1 knockdown inhibits the proliferation, migration, and invasion of NPC cells. (a) Transfect circFOXM1 siRNA into nasopharyngeal carcinoma cells. The expression levels of circFOXM1 and FOXM1 mRNA in the transfected and untransfected groups were detected by qPCR. (b) 5-8F and 6-10B cells were transfected with circFOXM1 siRNAs. The cell proliferation ability was detected by the CCK8 assay at the specified time points. (c) CircFOXM1 knockdown inhibited colony formation of both 5-8F and 6-10B cells. (d) Trans-well migration assay was used to detect the migration of circFOXM1-knockdown-transfected 5-8F and 6-10B cells. (e) Wound-healing assay to detect migration of circFOXM1-knockdown-transfected 5-8F and 6-10B cells. The error bars (e) represent the SD of three independent experiments. * $p < .05$, ** $p < .01$

by adsorbing a miRNA, thereby promoting the progression of NPC. We transfected cells with si-NC or si-circFOXM1 and extracted RNA. The results of qRT-PCR showed that after knocking down circFOXM1, the relative expression of miR-136-5p was significantly increased (Figure 3a). By retrieving TargetScan, StarBase, and other databases, we found that the binding sites of circFOXM1 and miR-136-5p are shown in Figure 3b. In order to further prove that circFOXM1 acts as a sponge to adsorb miR-136-5p, we conducted a dual-luciferase experiment. First, we constructed circFOXM1 WT and MUT dual-luciferase plasmids, transfected them into 5-8F and 6-10B cells, and then transfected them separately with NC mimics and miR-136-5p mimics, using a full spectrum microplate reader to detect the intensity of firefly/renilla fluorescein. The results show that miR-136-5p mimics can inhibit the luciferase activity of circFOXM1 WT, but has no effect on circFOXM1 Mut (Figure 3b). The dual-luciferase report experiment verified that circFOXM1 can bind to miR-136-5p. Therefore, we believe that CircFOXM1 can act as a sponge to adsorb miR-136-5p in NPC cells.

3.4 | MiR-136-5p regulates the proliferation and migration of NPC cells

In order to study the effect of miR-136-5p on NPC cells, we ordered inhibitors and mimics of miR-136-5p, respectively, transfected them into cells to extract RNA, and used qRT-PCR to detect the relative expression of miR-136-5p

(Figure 4a). We transfected miR-136-5p inhibitor and miR-136-5p mimics into 5-8F and 6-10B cells, respectively, and performed a set of cell function experiments. CCK8 experiments found that cells transfected with miR-136-5p inhibitor promote nasopharyngeal Cancer proliferation, transfection of miR-136-5p mimics can inhibit the proliferation of NPC (Figure 4b). In the clone formation experiment, it was found that the clone formation of NPC cells was reduced after miR-136-5p mimics were transfected, and the clone formation increased after the miR-136-5p inhibitor was transfected (Figure 4c). The histogram on the right is the quantification of the number of colonies. The wound-healing experiment found that after cells were transfected with miR-136-5p mimics, the cell migration ability decreased, hindering the healing of scratches. After NPC cells were transfected with miR-136-5p inhibitor, the cell migration ability was enhanced to promote the healing of scratches (Figure 4d). On the right is a quantitative histogram of cell migration rate.

3.5 | Knockdown of miR-136-5p can reverse the attenuation effect of si-circFOXM1-induced NPC cell proliferation, migration, and invasion

In previous experiments, we have proved that circFOXM1 can act as a sponge and adsorb miR-136-5p. In order to prove the effect of circFOXM1 on NPC cells after miR-136-5p adsorbed by circFOXM1, we transfected

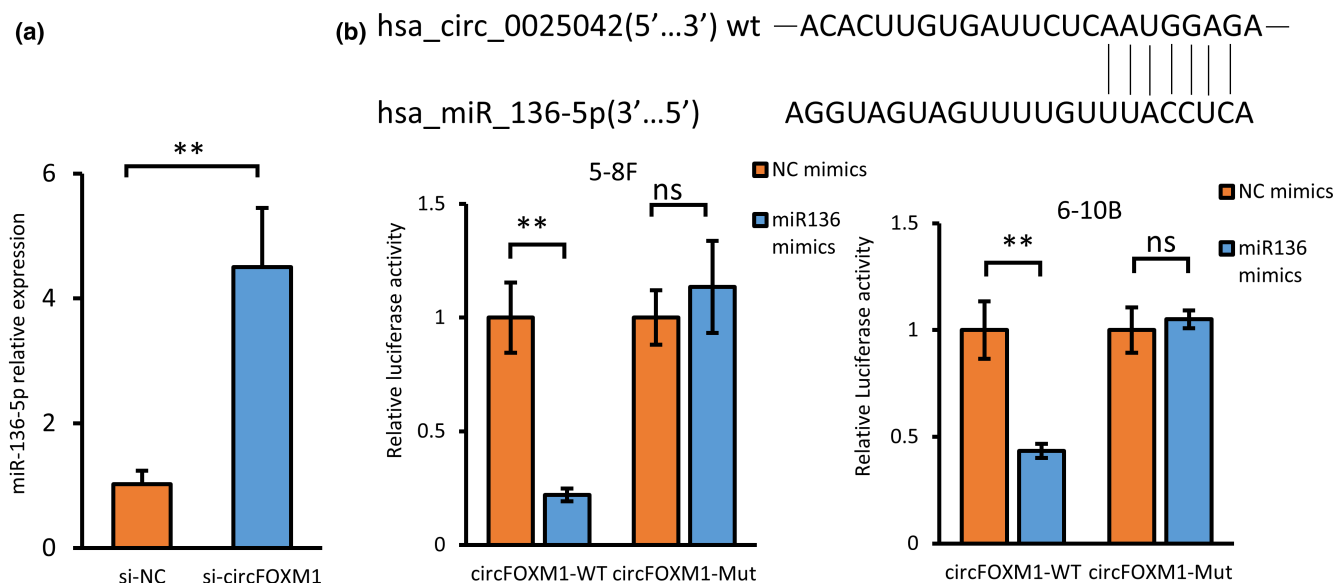


FIGURE 3 CircFOXM1 acts as a sponge for miR-136-5p in NPC cells. (a) The expression level of miR-136-5p was determined by qPCR after transfection of si-circFOXM1 in NPC cells. (b) Top panel: schematic diagram showing the predicted binding site of circFOXM1 and miR-136-5p. Bottom panel: luciferase activity was detected in 5-8F and 6-10B cells after being transfected with miR-136-5p mimic or miR-136-5p NC. The error bars (e) represent the SD of three independent experiments. * $p < .05$, ** $p < .01$

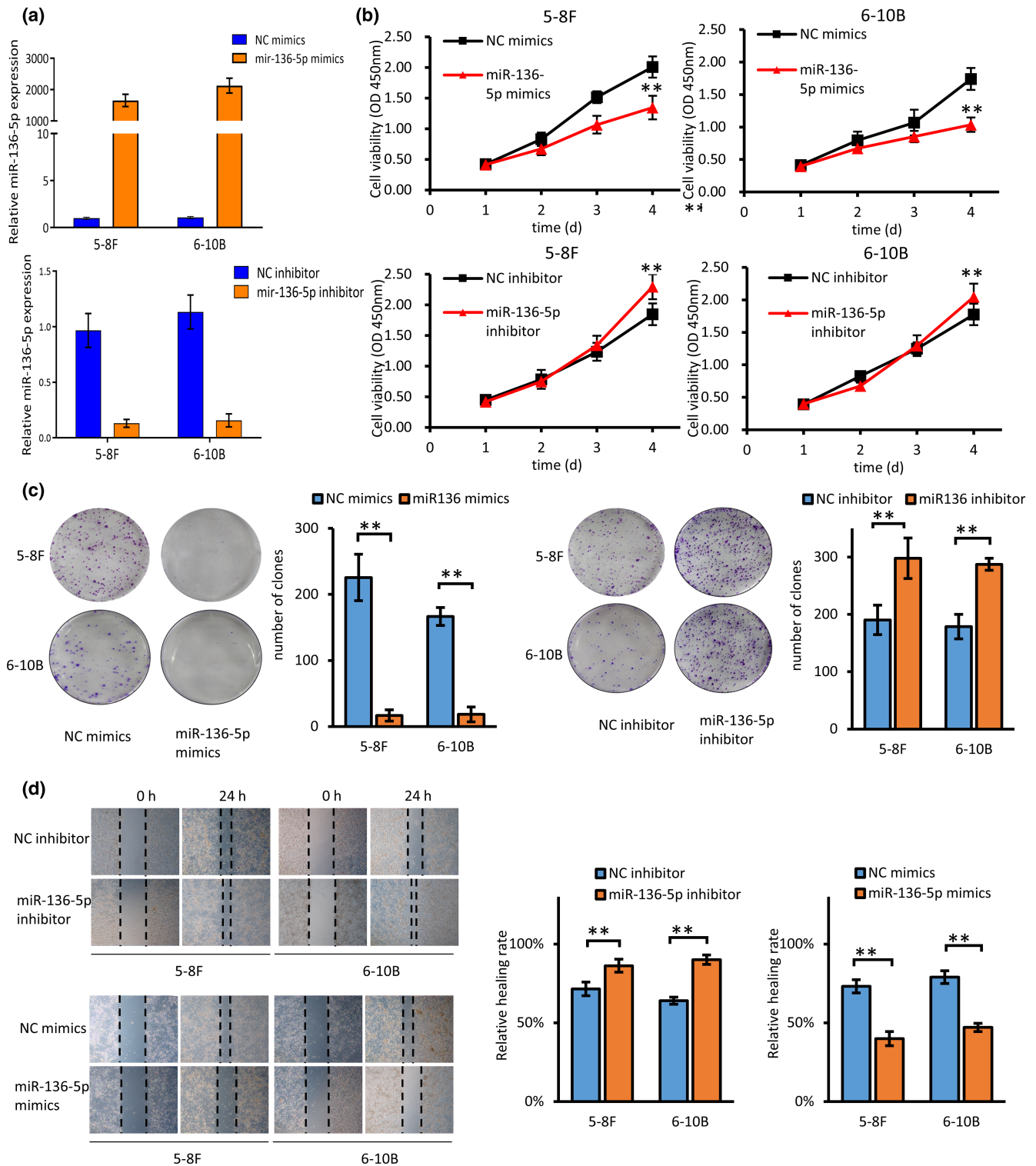


FIGURE 4 MiR-136-5p regulates the proliferation and invasion of NPC cells. 5-8F and 6-10B cells were transfected with control or miR-328-5p mimics or miR-136-5p inhibitors, and the proliferation, clone formation, and wound-healing experiments were examined. (a) The expressions of miR-136-5p after transfected with miR-328-5p mimics or miR-136-5p inhibitor were analyzed by qRT-PCR. (b) CCK-8 assay was performed to determine the viability in 5-8F and 6-10B cells with miR-136-5p mimics or miR-136-5p inhibitors. (c) The proliferative capacity of 5-8F and 6-10B cells transfected with miR-136-5p mimics or miR-136-5p inhibitors was evaluated by colony formation assay. (d) Cell migration was examined in NPC cells transfected with miR-136-5p mimics or miR-136-5p inhibitor by a wound-healing assay. The error bars (e) represent the SD of three independent experiments. $*p < .05$, $**p < .01$

si-circFOXM1 and miR-136-5p inhibitor into 5-8F and 6-10B cells, respectively, and cotransfected si-circFOXM1 and miR-136-5p inhibitor was used to conduct a set of cell function experiments on 5-8F and 6-10B cells. CCK8 experiments found that si-circFOXM1 inhibited the proliferation of NPC cells, miR-136-5p inhibitor promoted the proliferation of NPC cells, and had the effect of reversing si-circFOXM1 suppressing the proliferation of NPC cells (Figure 5a). Clone formation experiments showed that si-circFOXM1 reduced cell clone formation, miR-136-5p inhibitor increased cell formation, and had the effect of reversing si-circFOXM1's inhibition of NPC cell clone formation (Figure 5b). The results of wound-healing experiments indicated that the migration ability of cells was weakened after transfection of si-circFOXM1, and the migration ability of cells was enhanced after transfection of miR-136-5p inhibitor and could rescue the ability of si-circFOXM1 to inhibit the migration of NPC cells (Figure 5c). Trans-well experiments showed that cell invasion decreased after transfection of si-circFOXM1, increased cell invasion after transfection of miR-136-5p inhibitor, and could reverse the effect of si-circFOXM1 on NPC cell invasion (Figure 5d). The above experiments confirmed that circFOXM1 can enhance the proliferation, migration, and invasion of NPC by adsorbing miR-136-5p.

3.6 | CircFOXM1 regulates NPC EMT through miR-136-5p-SMAD2

Further studying the downstream target genes of miR-136-5p, we found that there have been studies showing that miR-136-5p can target *SMAD2/SMAD3* (OMIM accession number: 603109) and affect the EMT process of lung adenocarcinoma cells. We transfected miR-136-5p inhibitor and miR-136-5p mimics into 5-8F and 6-10B cells, respectively. After RNA extraction, the expression of circFOXM1 was detected by qRT-PCR and there was no noteworthy difference compared with the NC group (Figure 6a), indicating that miR-136-5p does not affect the expression of upstream circFOXM1. Then we tested the relative expression level of *SMAD2*. We discovered that the expression level of *SMAD2* decreased obviously after transfection of miR-136-5p mimics, and the expression level of *SMAD2* increased significantly after transfection of miR-136-5p inhibitor (Figure 6b). Then we transfected the cells with si-circFOXM1 and si-NC, and then extracted RNA to test the relative expression levels of *SMAD2* and *SMAD3*, respectively. We discovered that the expression level of *SMAD2* decreased dramatically after knocking down circFOXM1, while the

relative expression level of *SMAD3* was not significantly different (Figure 6c). We performed Western blot experiments with the extracted protein and discovered that the expression of *SMAD2* protein decreased obviously after circFOXM1 was knocked down, but there was no conspicuous difference in the expression of *SMAD3* protein (Figure 6d). In order to further study the regulatory relationship between circFOXM1 and *SMAD2*, we ordered circFOXM1 overexpression plasmid and si-SMAD2. We transfected cells with overexpression-circFOXM1 (OE-circFOXM1) plasmid to detect the expression of circFOXM1 to verify the effect of overexpression. We transfected si-SMAD2 into 5-8F and 6-10B cells and detected the relative expression of circFOXM1 by qRT-PCR. We found that there was no significant difference in the relative expression of circFOXM1 in these two cell lines (Figure 6e), which also indicated that *SMAD2* had no effect on the expression of upstream circFOXM1. We continue to study the mechanism by which circFOXM1 promotes the progression of NPC. EMT is epithelial-mesenchymal transition. During the transformation process, cells change from a tightly fixed state to a loosely migrating state. During this process, the synthesis of cell E-cadherin decreases, and the synthesis of N-cadherin, vimentin, etc. increased. We extracted 5-8F and 6-10B proteins and performed Western blot experiments to detect the expression of EMT-related proteins. We found that after knocking down circFOXM1, the expression of *SMAD2* protein, N-Cadherin, and Vimentin was significantly reduced, and the expression of E-Cadherin was significantly increased. The amount of expression increased significantly. When we cotransfected cells with si-circFOXM1 and miR-136-5p inhibitors, we found that the expression levels of *SMAD2* protein and EMT-related proteins were not significantly different from those of the control group (Figure 6f). From the above results, we proved that circFOXM1 affects the EMT process of NPC cells through the miR-136-5p-SMAD2 pathway and promotes the progress of NPC.

3.7 | OE-circFOXM1 reverses si-SMAD2 inhibition of NPC proliferation and invasion

In order to confirm the impact of *SMAD2* on the proliferation and invasion of NPC cells, we knocked down *SMAD2* and transfected the cells to perform functional experiments. We found that the proliferation ability of NPC cells was suppressed after knocking down *SMAD2* (Figure 7a). Then we conducted a rescue experiment, transfecting tumor cells with overexpressed circFOXM1

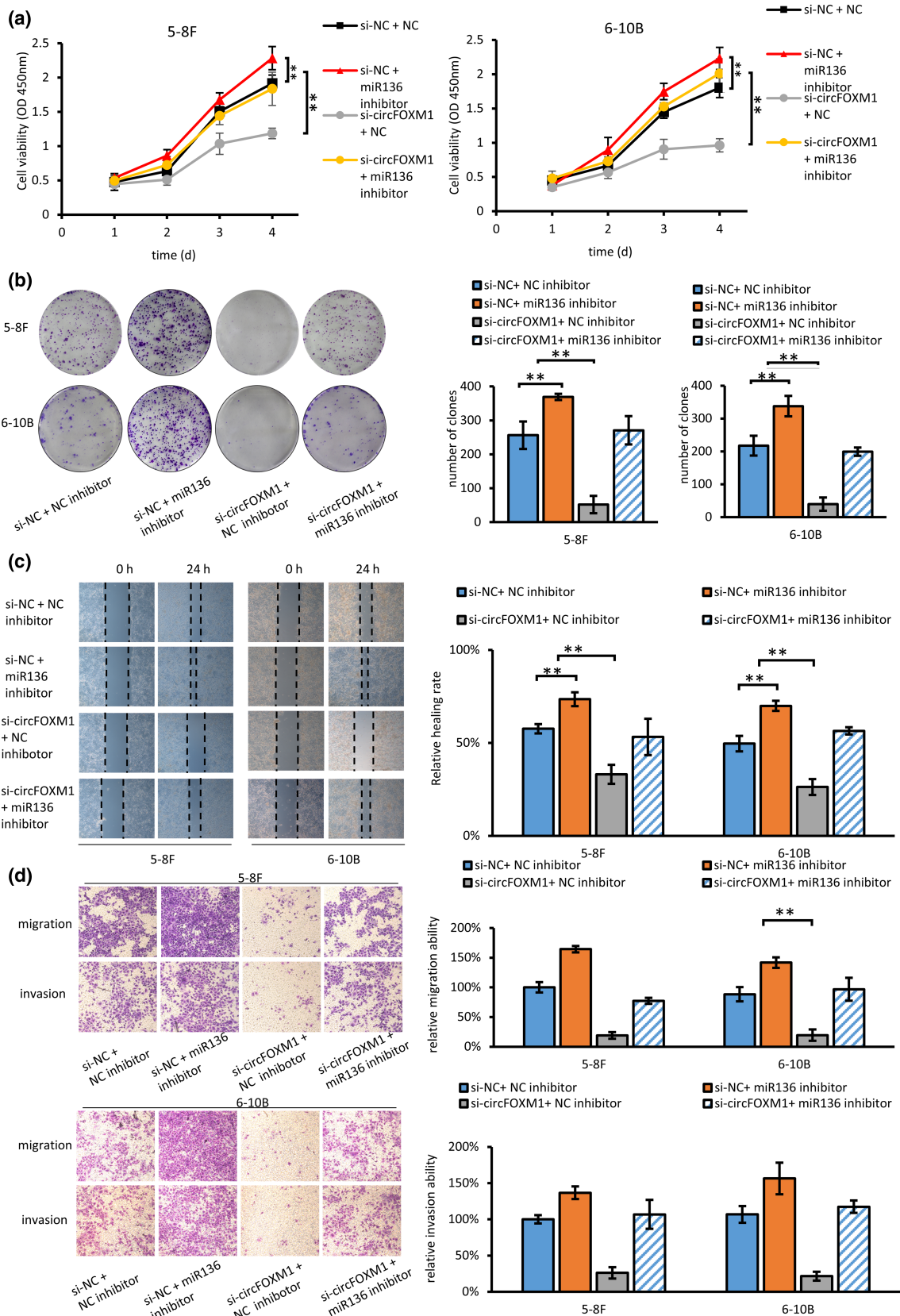


FIGURE 5 Knockdown of miR-136-5p reverses si-circFOXM1-induced the attenuation of cell proliferation, migration, and invasion in NPC cells. (a) 5-8F and 6-10B cells were transfected with si-circFOXM1 or miR-136-5p inhibitor or cotransfected with si-circFOXM1 and miR-136-5p inhibitor. Cell proliferation was determined by the CCK8 assay. (b) Colony formation assays were performed to assess the proliferative ability of 5-8F and 6-10B cells transfected with si-circFOXM1 or coransfected with si-circFOXM1 and miR-136-5p inhibitor. (c, d) Effects of si-circFOXM1 and miR-136-5p inhibitors on the migration and invasion of 5-8F and 6-10B cells were evaluated by wound-healing assay and trans-well migration assay. The error bars (e) represent the SD of three independent experiments. * $p < .05$, ** $p < .01$

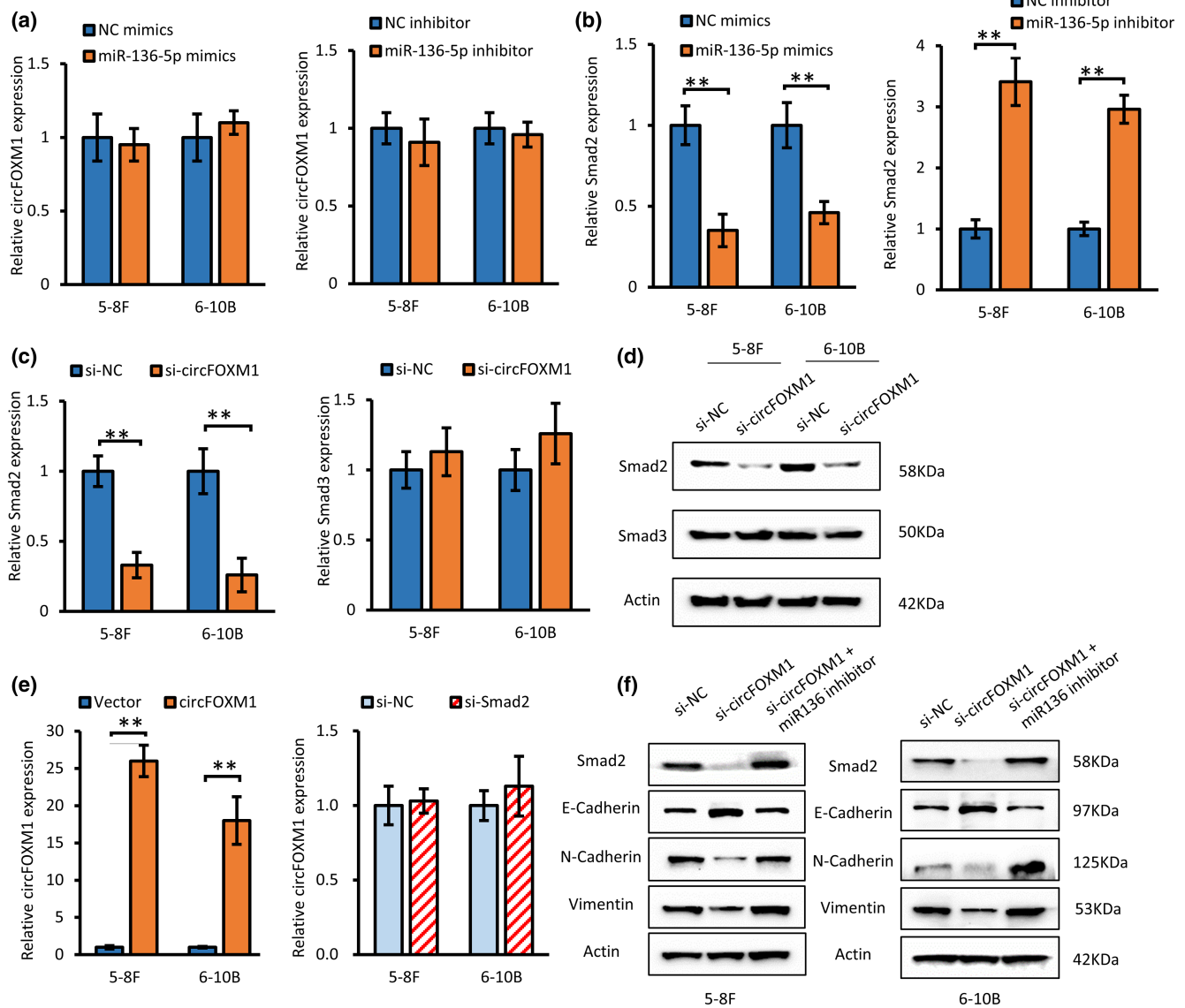


FIGURE 6 circFOXM1 regulates NPC EMT through miR-136-5p-SMAD2. (a) Relative expression of circFOXM1 after transfection of miR-136-5p mimics or miR-136-5p inhibitors. (b) Relative expression of SMAD2 after transfection of miR-136-5p mimics or miR-136-5p inhibitors. (c, d) Relative expression of mRNA and protein of *SMAD2* and *SMAD3* after transfection of si-circFOXM1. (e) Relative expression of circFOXM1 after transfection of OE-circFOXM1 and si-SMAD2. (f) MiR-136-5p inhibitors can reverse si-circFOXM1's inhibition of EMT-related protein expression. The error bars (e) represent the SD of three independent experiments. * $p < .05$, ** $p < .01$

to promote the proliferation of NPC. When overexpressed circFOXM1 and si-SMAD2 were used to transfect tumor cells together, we found that overexpressed circFOXM1 can reverse the inhibition of si-SMAD2 the role of NPC cell proliferation (Figure 7b). The wound-healing experiment found that si-SMAD2 inhibited the migration of NPC cells (Figure 7c), and overexpression of circFOXM1 could reverse the effect of si-SMAD2 on inhibiting the migration of NPC cells (Figure 7d). The clone formation experiment found that si-SMAD2 could reduce clone formation (Figure 7e), and overexpression of circFOXM1 could rescue the effect of si-SMAD2-inhibiting clone

formation (Figure 7f). Trans-well experiments found that si-SMAD2 inhibited cell invasion (Figure S1a), and OE-circFOXM1 could reverse the effect of si-SMAD2 on inhibiting invasion (Figure S1b). Si-SMAD2 could suppress the proliferation and invasion of NPC cells. CircFOXM1 promotes the proliferation, migration, and invasion of NPC cells through the circFOXM1-miR-136-5p-SMAD2 regulatory axis. In order to further confirm our conclusion, we transfected OE-SMAD2 and si-circFOXM1, respectively, and cotransfected 5-8F and 6-10B to do another set of functional experiments (Figure S2), and got the same conclusion.

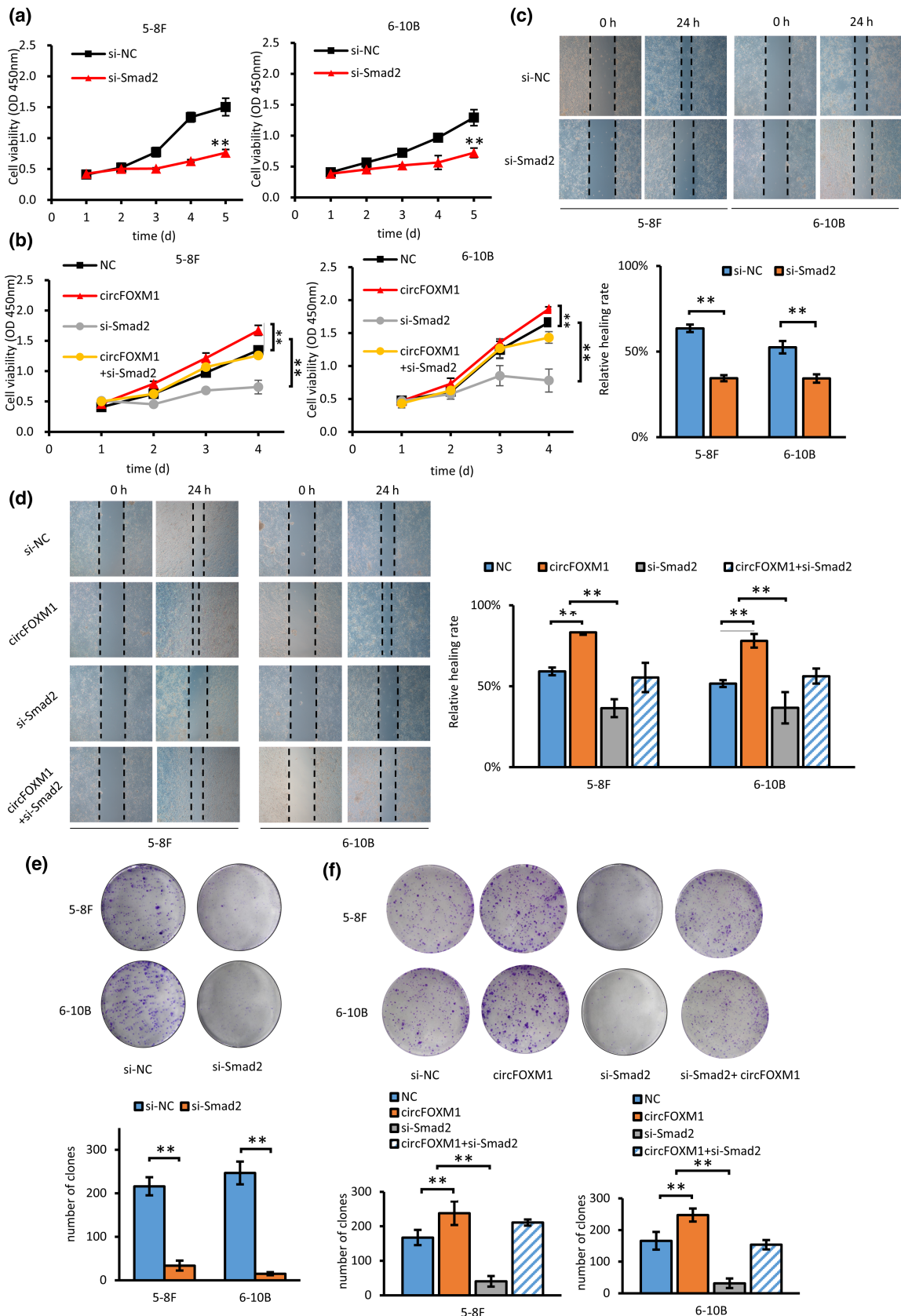


FIGURE 7 OE-circFOXM1 reverses si-SMAD2 inhibition of NPC proliferation and invasion. (a, b) CCK8 assays confirmed that si-SMAD2 inhibited cell proliferation, OE-circFOXM1 rescued si-SMAD2 inhibition of NPC proliferation. (c, d) Wound-healing assays confirmed that si-SMAD2 inhibited cell migration, OE-circFOXM1 rescued si-SMAD2 inhibition of NPC migration. (e, f) Colony formation assays were performed to assess the proliferative ability of 5-8F and 6-10B cells transfected with si-SMAD2 and OE-circFOXM1 or cotransfected with si-SMAD2 and OE-circFOXM1. The error bars (e) represent the SD of three independent experiments. * $p < .05$, ** $p < .01$

3.8 | Relative expression and correlation of circFOXM1, miR-136-5p, and SMAD2 in clinical samples

In order to study the expression and correlation of circFOXM1, miR-136-5p, and *SMAD2* in clinical NPC tissues, we collected 48 clinical samples, including 40 frozen NPC tissues and 8 normal nasopharyngeal epithelial tissues. We extracted RNA and detected by qRT-PCR that compared with normal tissues, the expression of circFOXM1 and *SMAD2* in NPC tissues increased, and the expression of miR-136-5p decreased (Figure 8a). We further performed the correlation analysis and found that the expression of miR-136-5p was negatively correlated with the expression of circFOXM1 and *SMAD2*, and the expression

of circFOXM1 was positively correlated with the expression of *SMAD2* (Figure 8b). We grouped the clinical samples of NPC by clinical stage and found that in the later clinical stage, the higher expression of circFOXM1 and *SMAD2*, the lower expression of miR-136-5p (Figure 8c). This shows that in clinical NPC tissue, the increased expression of circFOXM1 is related to clinical staging, which also indicates that circFOXM1 may become a possible target in the treatment of clinical NPC.

4 | DISCUSSION

In this research, we first found that circFOXM1 was up-regulated in NPC cells compared with adjacent tissues,

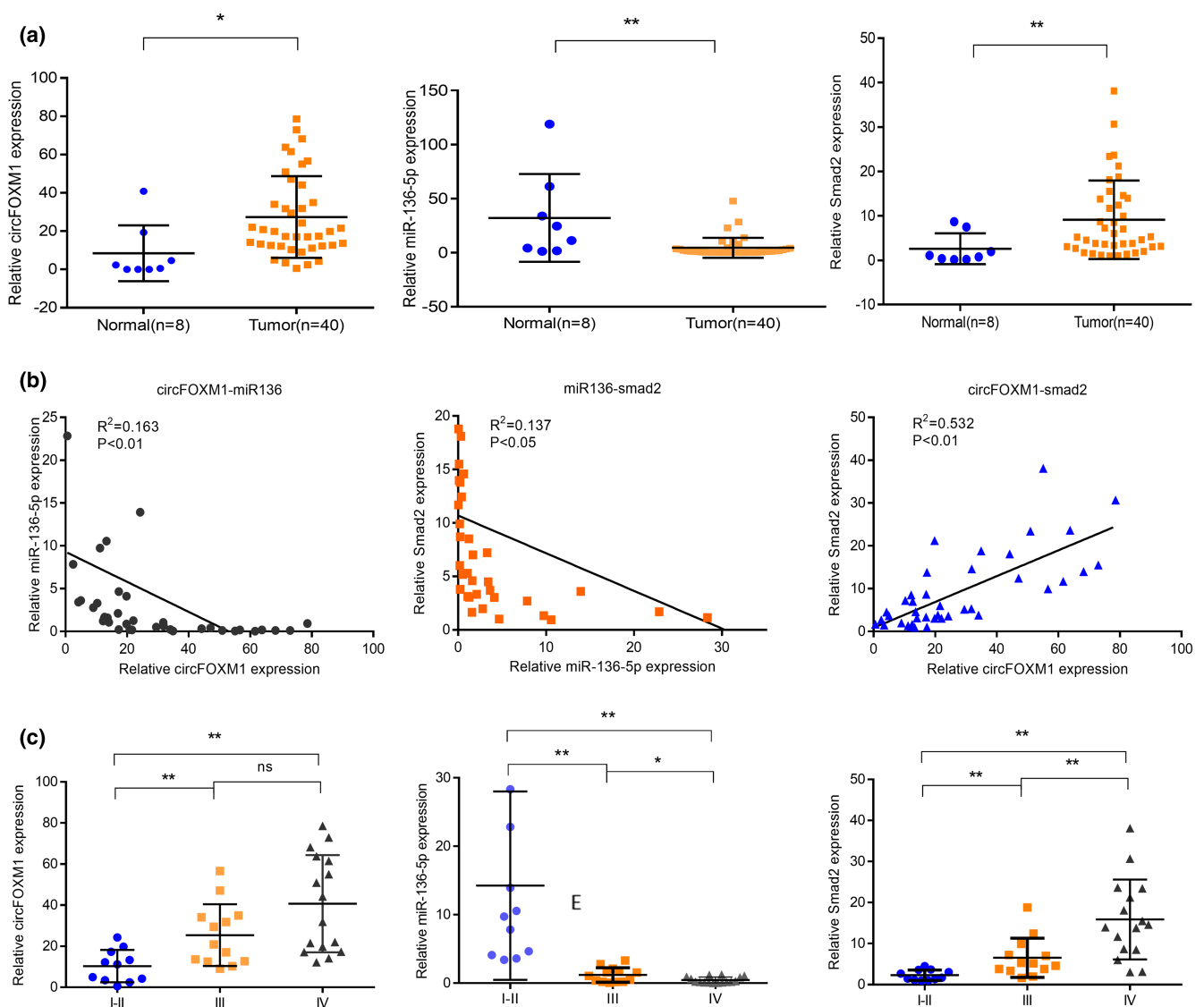


FIGURE 8 Relative expression and correlation of circFOXM1, miR-136-5p, and *SMAD2* in clinical samples. (a) Relative expression levels of circFOXM1, miR-136-5p, and *SMAD2* in clinical samples. (b) Linear correlation of relative expression of circFOXM1, miR-136-5p, *SMAD2*. (c) The relative expression levels of circFOXM1, miR-136-5p, and *SMAD2* in different clinical sample stages. The error bars (e) represent the SD of three independent experiments. * $p < .05$, ** $p < .01$

and its expression was significantly relevant to the clinical stage. Second, our statistical analysis data show that the expression of circFOXM1 is associated with the poor prognosis of patients, indicating that it may be promising as a biomarker for predicting the poor prognosis of NPC. Then, we proved that the overexpression of circFOXM1 reversed miR-136-5p's inhibitory effect on the proliferation and invasion of NPC, thereby promoting the development of NPC. Finally, we found that circFOXM1 acts as a ceRNA and regulates the expression of downstream *SMAD2* genes by competing with miR-136-5p to affect the EMT process of NPC (Yang et al., 2013). Considering the important role of circFOXM1 in the progression of NPC, our experimental results reveal the important significance of circFOXM1 in the treatment of NPC, indicating that it may be used as a biomarker for the diagnosis of NPC.

NPC is a relatively high incidence of malignant tumors in the head and neck malignancies, which is prone to local recurrence and distant metastasis (Hou et al., 2017). Due to the special anatomical location of NPC, the operation is difficult and risky, and NPC cells are sensitive to radiation, radiotherapy is still the first choice for NPC. In recent years, with the development of intensity-modulated

radiotherapy, the survival rate of NPC has been greatly improved (Chen et al., 2019), but some NPC patients still have the risk of distant metastasis and poor prognosis (Kang et al., 2017). Therefore, it is very meaningful to explore gene targets that can effectively treat NPC.

As a noncoding RNA, circRNA has been identified in the past few years. In recent years, many studies have discovered that circRNA plays a vital role in different physiological and pathological processes, especially carcinogenesis. Research on the role of circRNA as a biomarker in human cancer has attracted more and more attention (Wang, Yang, et al., 2018). For example, it promotes the proliferation and metastasis of lung adenocarcinoma (Qiu et al., 2018), liver cancer (Song et al., 2020) and cervical cancer (Ou et al., 2020). In previous studies, our group found that CircFOXM1 is obviously highly expressed in NPC tissues compared with normal nasopharyngeal tissues. However, there are few reports on the role of circRNA in the occurrence and development of NPC. We selected circFOXM1 in our research. CircFOXM1 is a circular RNA derived from the *FOXM1* gene. FOXM1 has become a key role in the development and progression of cancer. It is an effective effector and prognostic indicators (Borhani & Gartel, 2020). Ye

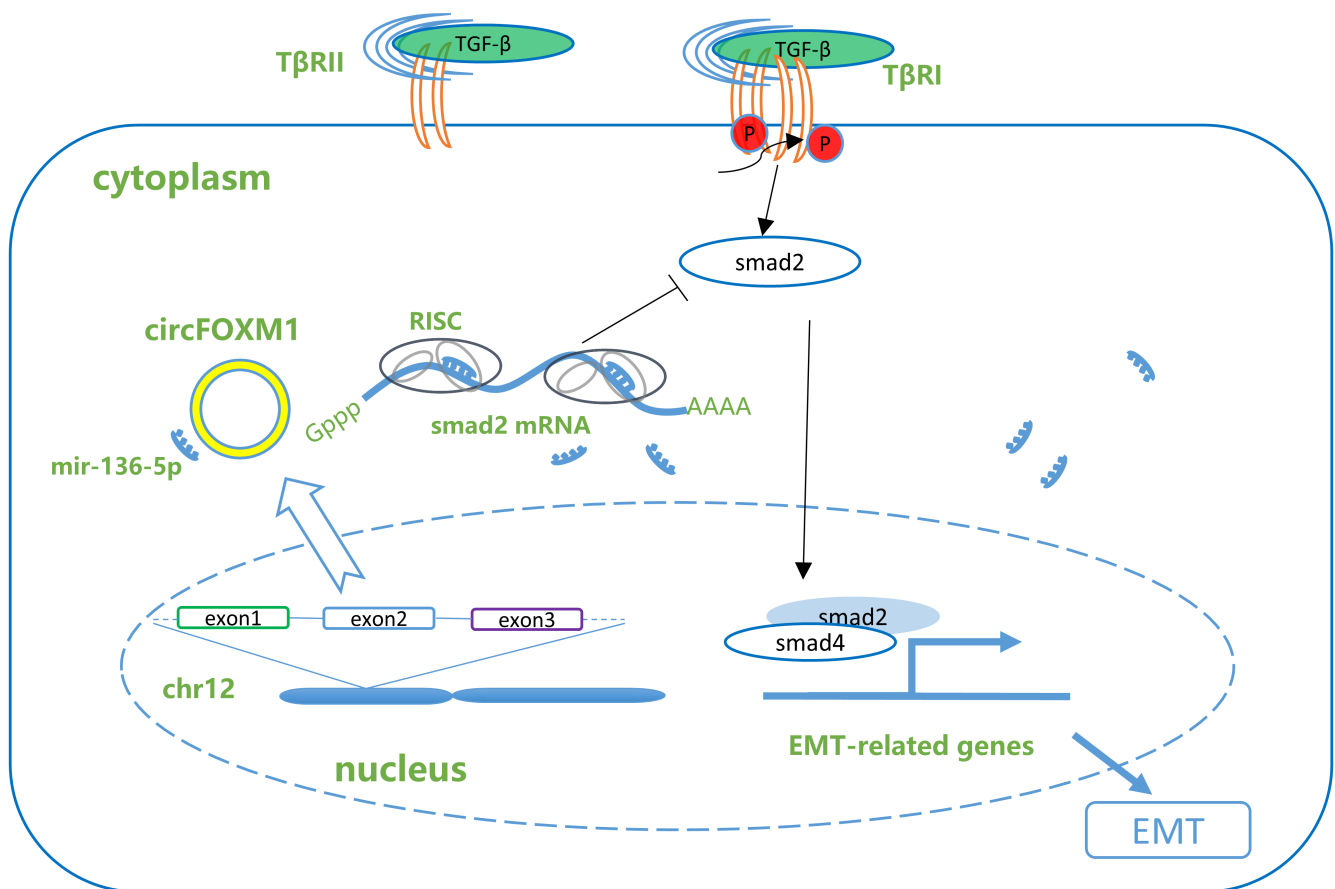


FIGURE 9 The schematic diagram shows that circFOXM1 acts as a sponge to adsorb miR-136-5p to regulate the expression of SMAD2, thereby promoting the proliferation and invasion of nasopharyngeal carcinoma cells

et al. found that circFOXM1 was upregulated in papillary thyroid carcinoma, and downregulation of circFOXM1 suppressed the tumor growth of papillary thyroid carcinoma in vitro and in vivo (Ye et al., 2020). Yu et al. reported that the expression of circFOXM1 was significantly upregulated in NSCLC tissues, and by combining with miR-614, it exerts its cancer-promoting effect (Yu et al., 2020). However, the molecular mechanism linking circRNA to the progression of NPC is still unclear. In our research, we studied the special molecular mechanism of circFOXM1 in NPC, and the results manifested that its expression was obviously upregulated in NPC cell lines and tissues, suggesting that circFOXM1 may be related to the development of NPC. Further experiments found that circFOXM1 is highly expressed in 5-8F and 6-10B cell lines, so we chose 5-8F 6-10B for follow-up experiments. si-NC and si-circFOXM1 were transfected into 5-8F and 6-10B cells to study the impact of circFOXM1 on the proliferation and invasion of NPC cells. We discovered si-circFOXM1 significantly inhibited the proliferation and invasion of 5-8F and 6-10B cells.

Overwhelming evidence have found that circRNA plays a significant role in the competitive endogenous RNA (ceRNA) network, which competitively binds to miRNA, thereby affecting the function of downstream miRNA target genes (Zhong et al., 2018). By searching databases such as TargetScan and Starbase, it was found that CircFOXM1 can bind to miR-136-5p, reducing the chance of miR-136-5p participating in the binding of the target gene silencing complex (Wang, Zhang, et al., 2018), thereby reversing the inhibitory effect of miR-136-5p on the target gene *SMAD2*. *SMAD2* is involved in signal transduction from cell surface receptors to the nucleus. In order to study the molecular mechanism of circFOXM1 in NPC, we used biological information to predict that miR-136-5p is a possible target of circFOXM1, and *SMAD2* is a downstream target gene of miR-136-5p (Yang et al., 2013). The results of dual-luciferase reporter gene experiment confirmed that miR-136-5p is indeed the target gene of circFOXM1 in NPC, and *SMAD2* is the target gene of miR-136-5p in NPC cells. In addition, we found a negative correlation between FOXM1 and miR-136-5p expression in NPC tissues, and a positive correlation between FOXM1 and *SMAD2* expression. Knockdown of FOXM1 significantly inhibited *SMAD2* expression, and miR-136-5p mimics exacerbated this inhibition. In summary, circFOXM1 acts as a sponge to adsorb miR-136-5p, promote the expression of *SMAD2* in NPC, and then promote the EMT process of NPC cells.

5 | CONCLUSION

In conclusion, our research shows that circFOXM1 acts as a molecular sponge to adsorb miR-136-5p in NPC tissues,

thereby reducing the binding of miR-136-5p to *SMAD2* and reducing the effect of inhibiting *SMAD2* expression. CircFOXM1 can promote the malignant proliferation and invasion of NPC cells by regulating the miR-136-5p/*SMAD2* axis (Figure 9). The circFOXM1-miR-136-5p-*SMAD2* regulatory pathway may become a clinical diagnosis or treatment target for NPC.

ACKNOWLEDGMENTS

We thank all members of the Radiotherapy Center of Jiangsu Cancer Hospital for their support and contributions. This study was supported by the National Science Foundation of China (grant numbers: 82003223, 81702685, and 8187101501) and the Postdoctoral Science Foundation of China (grant number: 2020 M671398).

CONFLICT OF INTEREST

The authors declare that they have no conflict of interest in this work.

ETHICAL STATEMENT

This study had been approved by Jiangsu Cancer Hospital Ethics Review Committee.

AUTHORS' CONTRIBUTIONS

Conceived and designed the experiments: Shuai Pei, Jie Chen, Mingyu Du, Chengxian Ma, Li Yin, and Xia He; Performed the experiments: Shuai Pei, Jie Chen, Xinyu Hu, and Chengxian Ma; Statistical analysis: Shuai Pei, Tian Xu, Mengna Zhan, Ke Xue, and Yufeng Zhang; Wrote the paper: Shuai Pei, Chengxian Ma, and Jie Chen. All authors read and approved the final manuscript.

DATA AVAILABILITY STATEMENT

The data that support the findings of this study are available from the corresponding author upon reasonable request.

ORCID

Shuai Pei  <https://orcid.org/0000-0001-8523-3484>

REFERENCES

- Borhani, S., & Gartel, A. (2020). FOXM1: A potential therapeutic target in human solid cancers. *Expert Opinion on Therapeutic Targets*, 24(3), 205–217.
- Chen, L., Zhang, Y., Lai, S., Li, W. F., Hu, W. H., Sun, R., Liu, L. Z., Zhang, F., Peng, H., Du, X. J., & Lin, A. H. (2019). 10-year results of therapeutic ratio by intensity-modulated radiotherapy versus two-dimensional radiotherapy in patients with nasopharyngeal carcinoma. *The Oncologist*, 24(1), e38–e45.
- Chua, M. L. K., Wee, J. T. S., Hui, E. P., & Chan, A. T. C. (2016). Nasopharyngeal carcinoma. *The Lancet*, 387(10022), 1012–1024.

- Ebbesen, K., Kjems, J., & Hansen, T. (2016). Circular RNAs: Identification, biogenesis and function. *Biochimica et Biophysica Acta*, 1859(1), 163–168.
- He, R., Hu, Z., Wang, Q., Luo, W., Li, J., Duan, L., Zhu, Y. S., & Luo, D. X. (2017). The role of long non-coding RNAs in nasopharyngeal carcinoma: As systemic review. *Oncotarget*, 8(9), 16075–16083.
- Hou, Y., Zhu, Q., Li, Z., Peng, Y., Yu, X., Yuan, B., Liu, Y., Liu, Y., Yin, L., Peng, Y., Jiang, Z., Li, J., Xie, B., Duan, Y., Tan, G., Gulina, K., Gong, Z., Sun, L., Fan, X., & Li, X. (2017). The FOXM1-ABCC5 axis contributes to paclitaxel resistance in nasopharyngeal carcinoma cells. *Cell Death & Disease*, 8(3), e2659.
- Kang, M., Zhou, P., Wei, T., Zhao, T., Long, J., Li, G., Yan, H., Feng, G., Liu, M., Zhu, J., & Wang, R. (2017). A new T staging system for nasopharyngeal carcinoma based on intensity-modulated radiation therapy: Results from a prospective multicentric clinical study. *American Journal of Cancer Research*, 7(2), 346–356.
- Lai, S. Z., Li, W. F., Chen, L., Luo, W., Chen, Y. Y., Liu, L. Z., Sun, Y., Lin, A. H., Liu, M. Z., & Ma, J. (2011). How does intensity-modulated radiotherapy versus conventional two-dimensional radiotherapy influence the treatment results in nasopharyngeal carcinoma patients? *International Journal of Radiation Oncology, Biology, Physics*, 80(3), 661–668.
- Lee, A. W., Ma, B. B., Ng, W. T., & Chan, A. T. (2015). Management of Nasopharyngeal Carcinoma: Current practice and future perspective. *Journal of Clinical Oncology: Official Journal of the American Society of Clinical Oncology*, 33(29), 3356–3364.
- Li, L. N., Xiao, T., Yi, H. M., Zheng, Z., Qu, J. Q., Huang, W., Ye, X., Yi, H., Lu, S. S., Li, X. H., & Xiao, Z. Q. (2017). MiR-125b increases nasopharyngeal carcinoma Radioresistance by targeting A20/NF-kappaB signaling pathway. *Molecular Cancer Therapeutics*, 16(10), 2094–2106.
- Liu, Z., Yu, Y., Huang, Z., Kong, Y., Hu, X., Xiao, W., Quan, J., & Fan, X. (2019). CircRNA-5692 inhibits the progression of hepatocellular carcinoma by sponging miR-328-5p to enhance DAB2IP expression. *Cell Death & Disease*, 10(12), 900.
- Luo, Z., Rong, Z., Zhang, J., Zhu, Z., Yu, Z., Li, T., Fu, Z., Qiu, Z., & Huang, C. (2020). Circular RNA circCCDC9 acts as a miR-6792-3p sponge to suppress the progression of gastric cancer through regulating CAV1 expression. *Molecular Cancer*, 19(1), 86.
- Mai, S., Xiao, R., Shi, L., Zhou, X. M., Yang, T., Zhang, M. Y., Weng, N. Q., Zhao, X. G., Wang, R. Q., Liu, J., Sun, R., Qin, H. D., & Wang, H. Y. (2019). MicroRNA-18a promotes cancer progression through SMG1 suppression and mTOR pathway activation in nasopharyngeal carcinoma. *Cell Death & Disease*, 10(11), 819.
- Ou, R., Mo, L., Tang, H., Leng, S., Zhu, H., Zhao, L., Ren, Y., & Xu, Y. (2020). circRNA-AKT1 sequesters miR-942-5p to upregulate AKT1 and promote cervical cancer progression. *Molecular Therapy Nucleic Acids*, 20, 308–322.
- Qiu, M., Xia, W., Chen, R., Wang, S., Xu, Y., Ma, Z., Xu, W., Zhang, E., Wang, J., Fang, T., Hu, J., Dong, G., Yin, R., Wang, J., & Xu, L. (2018). The circular RNA circPRKCI promotes tumor growth in lung adenocarcinoma. *Cancer Research*, 78(11), 2839–2851.
- Qu, J., Li, M., Zhong, W., & Hu, C. (2015). Competing endogenous RNA in cancer: A new pattern of gene expression regulation. *International Journal of Clinical and Experimental Medicine*, 8(10), 17110–17116.
- Qu, S., Zhong, Y., Shang, R., Zhang, X., Song, W., Kjems, J., & Li, H. (2017). The emerging landscape of circular RNA in life processes. *RNA Biology*, 14(8), 992–999.
- Salmena, L., Poliseno, L., Tay, Y., Kats, L., & Pandolfi, P. (2011). A ceRNA hypothesis: The Rosetta stone of a hidden RNA language? *Cell*, 146(3), 353–358.
- Song, L., Qiao, G., Yu, J., Yang, C. M., Chen, Y., Deng, Z. F., Song, L. H., Ma, L. J., & Yan, H. L. (2020). Hsa_circ_0003998 promotes epithelial to mesenchymal transition of hepatocellular carcinoma by sponging miR-143-3p and PCBP1. *Journal of Experimental & Clinical Cancer Research: CR*, 39(1), 114.
- Wang, M., Yang, Y., Xu, J., Bai, W., Ren, X., & Wu, H. (2018). CircRNAs as biomarkers of cancer: A meta-analysis. *BMC Cancer*, 18(1), 303.
- Wang, M., Zhang, L., Liu, Z., Zhou, J., Pan, Q., Fan, J., Zang, R., & Wang, L. (2018). AGO1 may influence the prognosis of hepatocellular carcinoma through TGF- β pathway. *Cell Death & Disease*, 9(3), 324.
- Yang, Y., Liu, L., Cai, J., Wu, J., Guan, H., Zhu, X., Yuan, J., Chen, S., & Li, M. (2013). Targeting SMAD2 and SMAD3 by miR-136 suppresses metastasis-associated traits of lung adenocarcinoma cells. *Oncology Research*, 21(6), 345–352.
- Ye, M., Hou, H., Shen, M., Dong, S., & Zhang, T. (2020). Circular RNA circFOXM1 plays a role in papillary thyroid carcinoma by sponging miR-1179 and regulating HMGB1 expression. *Molecular Therapy Nucleic Acids*, 19, 741–750.
- Yu, C., Cheng, Z., Cui, S., Mao, X., Li, B., Fu, Y., Wang, H., Jin, H., Ye, Q., Zhao, X., Jiang, L., & Qin, W. (2020). circFOXM1 promotes proliferation of non-small cell lung carcinoma cells by acting as a ceRNA to upregulate FAM83D. *Journal of Experimental & Clinical Cancer Research: CR*, 39(1), 55.
- Zheng, Z., Li, Z., Zhou, G., Lin, L., Zhang, L. L., Lv, J. W., Huang, X. D., Liu, R. Q., Chen, F., He, X. J., & Kou, J. (2019). Long non-coding RNA FAM225A promotes nasopharyngeal carcinoma tumorigenesis and metastasis by acting as ceRNA to sponge miR-590-3p/miR-1275 and upregulate ITGB3. *Cancer Research*, 79(18), 4612–4626.
- Zhong, Y., Du, Y., Yang, X., Mo, Y., Fan, C., Xiong, F., Ren, D., Ye, X., Li, C., Wang, Y., & Wei, F. (2018). Circular RNAs function as ceRNAs to regulate and control human cancer progression. *Molecular Cancer*, 17(1), 79.

SUPPORTING INFORMATION

Additional supporting information may be found in the online version of the article at the publisher's website.

How to cite this article: Pei, S., Ma, C., Chen, J., Hu, X., Du, M., Xu, T., Zhan, M., Xue, K., Zhang, Y., Yin, L. & He, X. (2022). CircFOXM1 acts as a ceRNA to upregulate SMAD2 and promote the progression of nasopharyngeal carcinoma. *Molecular Genetics & Genomic Medicine*, 10, e1914. <https://doi.org/10.1002/mgg3.1914>